Is 1T the new 9.4T? A tool for morphological phenotyping and regional brain volume extraction

Holly Elizabeth Holmes*[1], Rajiv Ramasawmy[1], Da Ma[1,2], Nicholas Powell[1,2], Manuel Jorge Cardoso[2], Marc Modat[2], Simon Walker-Samuel[1], Sebastian Ourselin[2], Bernard Siow+[1,2], and Mark Lythgoe+[1]

[1]*Centre for Advanced Biomedical Imaging, University College London, London, Greater London, United Kingdom,* [2]*Centre for Medical Image Computing, University College London, London, Greater London, United Kingdom*

**Joint first authors; +Joint senior authors*

Introduction

Recently low-field MRI scanners, specifically designed for preclinical imaging, have come to market.[1] These so-called 'bench-top' scanners are compact, do not require cryogen-cooling, have no stray field, and may serve as an economical alternative to high-field scanners. The question remains as to the best use of these scanners, and whether they can replace the more expensive high-field systems. One possible application is high throughput 3D mouse brain phenotyping projects, where MRI has already established itself as a valuable tool, as their small footprint means they can be placed in most biomedical research centres and they require no specialist MRI knowledge to operate. However, it is still unclear whether these bench-top systems, with compromised signal (SNR) and contrast-to-noise ratio (CNR), are suitable for morphological characterisation of mutant mice. In this work, we sought to compare low (1T) with high-field (9.4T) MRI for calculating regional brain volumes (based on automated structural parcellation[2]) in a cohort of wildtype mice, comparing time-matched high-resolution acquisitions to that of a high-field system.[3]

Methods

Sample preparation: 6 wildtype C57BL/6 mice were terminally anaesthetised with Euthanal administered via intraperitoneal injection. The thoracic cavities were opened and the animals were intracardially perfused through the left ventricle: first with 15 – 20 mL of saline (0.9%) and heparin; second with 50 mL of buffered formal saline and 8 mM Magnevist, at a flow rate of 3 mL per minute. Following perfusion, the animal was decapitated, defleshed, and the lower jaw removed. All brains were stored in-skull at 4 ^{o}C and soaked in buffered formal saline and 8 mM Magnevist for at least 9 weeks prior to *ex vivo* scanning. Sequence optimisation*: T_1 & T_2* mapping at 1T:* Single slice, coronal, gradient echo (FLASH), 96^2 matrix, FOV 20 mm^2, slice thickness 1 mm, TR 300 s, TE 3 ms, Flip Angle 45°. *For T_1 mapping,* 11 exponentially spaced Tis followed an adiabatic inversion, and for *T_2* mapping 8* echoes were spaced by 5 ms. Optimal scan parameters were estimated by adapting the method outlined by Cleary et al which optimised CNR.[3] For our study we optimised parameters for good contrast between the corpus callosum and cortex. High resolution structural imaging: *Agilent 9.4T VNMRS* (Agilent Technologies, CA, USA). 3D gradient echo sequence, isotropic 40µm voxels, TE 4.5ms, TR 17s, flip angle 51°, 6 averages, acquisition time 11 hours 38 minutes.[3] *Bruker 1.0T ICON* (Bruker BioSciences Corporation, Ettlingen, Germany). 3D navigated gradient echo (IntraGate FLASH), isotropic 80µm voxels, TE 10 ms, TR 20 ms, , flip angle 61°, 22 averages, acquisition time 11 hours 54 minutes. Image Analysis*: T_1* and *T_2** maps were generated across the regions of interest in MATLAB (MathWorks, USA) using pixel-wise 3 and 2 parameter curve fits respectively. SNR was estimated from the mean signal magnitude within a cortical ROI to the variance of Rayleigh-distributed background noise.[4] CNR was measured as the difference in SNR between the cortical tissue and corpus callosum. After separation from multiple-subject images and orientation to standard space[5], brains were automatically parcellated with a multi-atlas-based approach,[2, 6-8] using an external mouse brain atlas.[8]

Table 1 T1 and T_2* relaxation times for the cortex and corpus callosum at 1T

Cortex		Corpus callosum	
T1	*T_2**	*T1*	*T_2**
36.3	16.9	38.0	14.6

Table 2 Calculating the mean cortical SNR and grey/white matter CNR at 1T and 9.4T

	1T	9.4T
SNR	15.0	15.4
GM/WM CNR	6.0	7.5

Results

T_1 and T_2* relaxation times at 1T were calculated for the cortex and corpus callosum in order to optimise the *ex vivo* imaging protocol for good grey/white matter contrast (Table 1). Following optimisation of the 1T sequence, high resolution structural images were acquired for 6 wildtype animals at both high and low-field. Figure 1 shows a single coronal slice taken from a representative wildtype animal at 1T and 9.4T. While the 9.4T images appear noticeably improved, there is no marked improvement in SNR over 1T (Table 1). The 9.4T images do, however, show improvements in CNR (from 6 to 7.5) (Table 2). The results from the automated structural parcellation[2] are shown in Table 3. Importantly, we observed good correspondence between volumes extracted from the 9.4T and the 1T data, with no significant differences detected between the two systems.

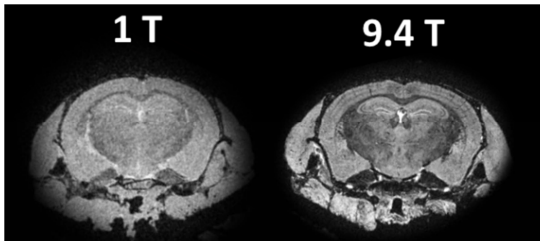

Figure 1 High resolution structural images taken at 1T

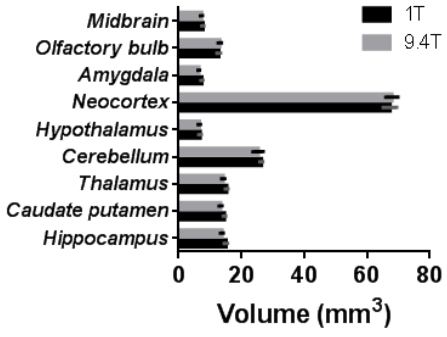

Table 3 1 Absolute volumes for brain structures extracted from the 1T and 9.4T data

Discussion

The similarity of SNR and CNR values is likely due to the larger voxel size and increased averaging, however the time-matched imaging protocol at 1T shows no apparent detriment to volumetry fidelity. Our encouraging results illustrate the application of low-field MRI for high throughput phenotyping in mice. The regions reported are commonly affected in neurodegenerative diseases and thus we hope to further explore potential uses of the 1T system by imaging a cohort of transgenic animals, to assess the sensitivity of low-field MR to morphometric changes.

REFERENCES: [**1**] Schmid, A., J. Schmitz, et al. (2013) *Molecular Imaging and Biology* 15(2): 155-165 [**2**] Ma, D., M. J. Cardoso, et al. (2014) *PLoS ONE* 9(1) [**3**] Cleary, J. O., F. K. Wiseman, et al. (2011) *NeuroImage* 56(3): 974-983 [**4**] Walker-Samuel, S., M. Orton, et al. (2009) *Magnetic Resonance in Medicine* 62(2): 420-429 [**5**] Powell, N. (2013). *ESMRMB Proceedings* (software) 699 [**6**] Ourselin, S., A. Roche, et al. (2000) *MICCAI* 2000 1935: 557-566. [**7**] Modat, M., G. R. Ridgway, et al. (2010) *Computer Methods and Programs in Biomedicine* 98(3): 278-284 [**8**] Jorge Cardoso, M., K. Leung, et al. (2013) *Medical Image Analysis* 17(6): 671-684 [**9**] Ma, Y., P. R. Hof, et al. (2005) *Neuroscience* 135(4): 1203-1215.